Superplasticity and High Strength in Al–Zn–Mg–Zr Alloy with Ultrafine Grains

Ruslan Z. Valiev,* Vil U. Kazykhanov, Aydar M. Mavlyutov, Anna A. Yudakhina, Nguyen Q. Chinh, and Maxim Yu Murashkin

Herein, the ultrafine-grained (UFG) 7xxx series alloy Al–4.8Zn–1.2Mg–0.14Zr demonstrates superplasticity at unusually low temperatures of 120–170 °C while maintaining its high-strength state. The UFG structure is formed by high pressure torsion (HPT) at room temperature (RT), which leads to a considerable increase in the strength characteristics by $\approx$60% compared with the material after conventional heat treatment T6. It is found that the UFG alloy exhibits thermostability when testing or annealing up to 170 °C. Deforming by tensile test at a strain rate of $10^{-4}\,s^{-1}$ and $10^{-3}\,s^{-1}$, the elongation to failure at 120 and 170 °C exceeds 250% and 500%, respectively, whereas the strain rate sensitivity reaches 0.45, which is a typical value characterizing superplastic deformation. After superplastic deformation, the UFG alloy maintains 25–50% higher strength characteristics at RT than that after conventional heat treatment T6. The origin of such superior behavior of the UFG alloy is discussed.

1. Introduction

Superplasticity (SP) of crystalline (metallic, ceramic, and composite) materials is one of the favorite subjects that Prof. Terence G. Langdon is most responsible for bringing into the scientific mainstream. His first works on SP published in 1977;[1,2] then, Langdon and co-workers have authored over 100 publications on this subject, including review articles[3–5] actually developing very important insights about the nature of this phenomenon. As an active member and Chairman (1991–1997) of the International Committee on Superplasticity, Langdon gave an impulse to encourage the studies of SP in leading laboratories worldwide. His earlier scientific results include the first

Prof. R. Z. Valiev, Dr. V. U. Kazykhanov, A. A. Yudakhina,
Dr. M. Y. Murashkin
Institute of Physics of Advanced Materials
Ufa State Aviation Technical University
12 K. Marx Street, Ufa 450008, Russia
E-mail: ruslan.valiev@ugatu.su

Prof. R. Z. Valiev, Dr. A. M. Mavlyutov
Saint Petersburg State University
Universitetskiy prospekt 28, Peterhof, St. Petersburg 198504, Russia

Prof. N. Q. Chinh
Department of Materials Physics
Eötvös Loránd University
Pázmány Péter sétány 1/A., H-1117 Budapest, Hungary

The ORCID identification number(s) for the author(s) of this article can be found under https://doi.org/10.1002/adem.201900555.

DOI: 10.1002/adem.201900555

experimental evidence for the occurrence of cavitation in superplastic flow[1] and set a world record of >5000% elongation in a lead–tin alloy:[2] this exciting result was listed for several years in the "Guinness Book of Records." It is well known that SP is associated with grain boundary sliding (GBS) and with attempts to determine the role of GBS. Vastava and Langdon undertook the first experimental measurements of the GBS contributions from intercrystalline and interphase boundaries in a superplastic alloy.[6] When later Langdon returned to the problem of grain boundary behavior, he developed a theoretical model of GBS, which combined both creep and superplastic conditions.[7]

Emergence of the subject of ultrafine-grained (UFG) metals produced by severe plastic deformation (SPD) techniques[8,9] and revealing their unusual mechanical behavior prompted Langdon to give more attention to the new topic of SP of the UFG metals and alloys, and the authors are glad to mark a number of pioneering works performed and published in collaboration with Terry on establishing high strain rate SP of UFG materials, study of the mechanisms of unusual behavior of these materials,[10,11] and so on.

This article is also devoted to the study of SP of UFG materials. For the first time, it presents the results on SP in the UFG aluminum alloy that demonstrates very high strength at room temperature (RT). It will be also shown that after superplastic deformation, the investigated UFG alloy maintains high strength, which is significantly higher than that in the coarse-grained condition after conventional heat treatment T6.

2. Experimental Section

In this work aluminum alloy of the 7xxx series was used as the material for study with chemical composition as follows: Al–4.8Zn–1.2Mg–0.14Zr (wt%). Disc-shaped samples (diameter 20 mm, thickness 1.4 mm) were cut out from the extruded rods for SPD processing using high pressure torsion (HPT). Following the previous studies,[12,13] the alloy was homogenized at 470 °C for 1 h and water-quenched immediately before HPT processing. The samples were subsequently processed by HPT for ten revolutions at RT under a hydraulic pressure of 6 GPa and at a ram rotation speed of 1 rpm. As was shown in earlier works,[14,15] such HPT processing conditions for aluminum

**ADVANCED
SCIENCE NEWS**

www.advancedsciencenews.com

**ADVANCED
ENGINEERING
MATERIALS**

www.aem-journal.com

alloys of the 7xxx series allow forming a uniform UFG structure and achieving very high values of strength.

All investigations on the microstructure and mechanical properties of the alloy were performed near the half radius of the disc samples.

A number of initial samples were subjected to conventional heat treatment T6 that is recommended for achieving maximum hardening in the 7xxx series alloys.[16] This treatment included a solution heat treatment at 470 °C for 2 h followed by water quenching to introduce a supersaturated solid solution and aging at 120 °C for 24 h.

Thermal stability of the HPT-processed alloy samples was also studied. It was recently shown that,[17] after HPT processing at RT, the UFG alloy 7475 maintains a rather high level of strength after annealing for 1 h at a temperature of 200 °C. Considering the earlier results, the present HPT-processed samples were annealed in the temperature range of 90–200 °C for 1 h.

Transmission electron microscopy (TEM) studies were conducted using JEOL JEM-2100 electron microscope at an accelerating voltage of 200 kV. Observations were made in the bright- and dark-field imaging modes, and selected area electron diffraction (SAED) patterns were recorded from areas of interest using an aperture of a 1 μm nominal diameter. To study the microstructure, thin foils were used, produced by jet polishing on a Tenupol-5 machine with the chemical solution consisting of 20% nitric acid and 80% methanol at a temperature of −25 °C and a voltage of 15 V. A mean grain size was determined based on the measurements of at least 200 mean diameters. At least three foils of each state were studied to obtain statistically relevant results.

Vickers microhardness (HV) was measured using a Shimadzu HMV-G microindentation tester with a load of 1 N for a dwell time of 15 s. Tensile tests were conducted on the test machine Instron 5982. The tests were computer controlled, recording the temperature, strain ε, and stress σ. The mechanical tests of the alloy samples with a gauge part of $2.0 \times 1.0 \times 0.8$ mm were conducted at RT, 120, 150, and 170 °C in the range of strain rate $\dot{\varepsilon}$ of 10^{-1}–10^{-4} s^{-1}. The results of tensile tests at RT were used to determine the characteristics of strength (yield stress [σ_{YS}] and ultimate tensile strength [σ_{UTS}]) and ductility (elongation to failure [δ]) of the samples after HPT and after conventional hardening treatment T6. Following the results of tensile tests of the UFG alloy in the temperature range of 120–170 °C, the value of strain rate sensitivity m was determined using the $m = \frac{\partial \ln\sigma}{\partial \ln\dot{\varepsilon}}$ definition.

3. Results

3.1. Grain Refinement and Thermal Stability

HPT processing of the alloy Al–4.8Zn–1.2Mg–0.14Zr at RT led to the formation of the UFG structure, as shown in **Figure 1**a. Quantitative analysis showed that the mean grain size was 176 ± 13 nm. As is seen from SAED (Figure 1a), the grains are separated by boundaries with mostly high-angle misorientations. The noted features of the UFG structure are the characteristics of many aluminum alloys subjected to HPT processing at similar regimes.[14,17] TEM images of the UFG structure could not reveal the formation of dispersed particles of secondary phases, nanosized clusters, and/or atom segregations of alloying elements. Such nanostructural features were only
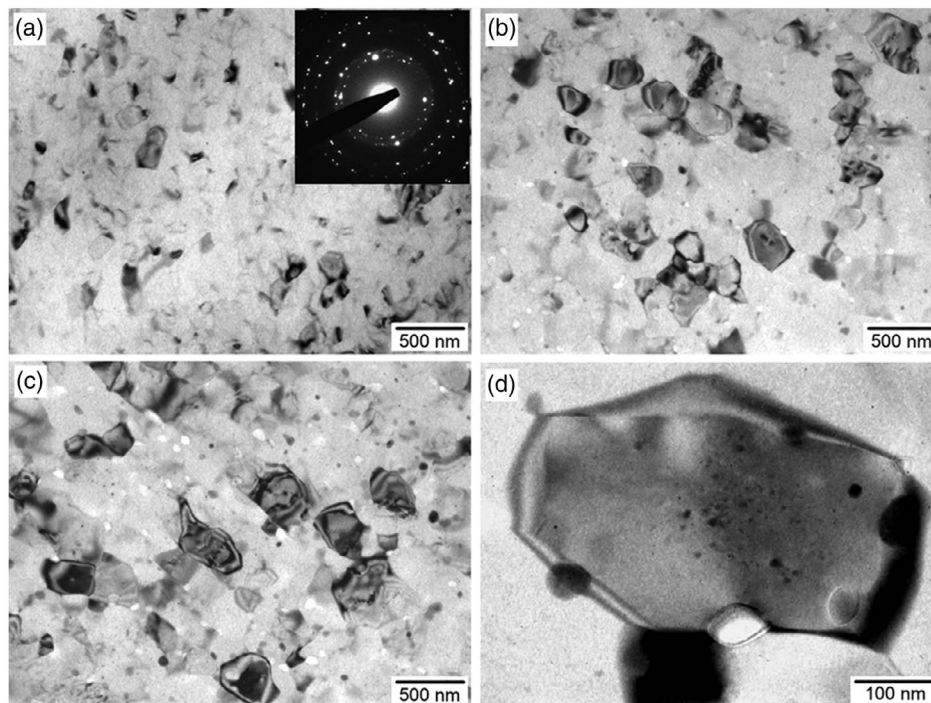
Figure 1. TEM images of UFG Al alloy after HPT at a) RT and further annealing at b) 150 and c,d) 170 °C correspondingly.

recently identified in the 7xxx series alloys processed by HPT under similar conditions, using more precise methods of scanning transmission electron microscopy (STEM) and 3D atom probe tomography (APT).[17,18] Apparently, such nanosized elements are also present in the microstructure of the HPT-processed supersaturated Al–4.8Zn–1.2Mg–0.14Zr alloy, but their observation requires the use of higher resolution systems. It is well known that the presence of nanosized particles, clusters, and grain-boundary segregations in the UFG structure makes it possible to achieve a unique level of strength by additional hardening mechanisms associated with these nanostructural features characterizing SPD-processed alloys.[14,17,18] This explains the fact that after HPT at RT, the microhardness (HV = 186 ± 7) of the UFG alloy Al–4.8Zn–1.2Mg–0.14Zr exceeded by ≈80% the microhardness (HV = 102 ± 5) of the sample after conventional heat treatment T6 (**Figure 2**).

In the UFG structure of the alloy, no noticeable change in the mean grain size after annealing for 1 h at 120 °C was observed. The grain size is 197 ± 10 nm. The changes in the UFG structure became more significant with a rise in the annealing temperature (Figure 1b,c). After annealing at 150, 170, and 200 °C, the mean grain size of the alloy increased to 223 ± 16, 294 ± 12, and 385 ± 11 nm, respectively. In addition to the coarsening of the ultrafine grains in the annealing microstructure, the formation of nanosized particles was observed besides the original Al_3Zr particles having a size of 20–30 nm. Quantitative analysis showed that the mean size of the coarse particles formed in the grain boundary region with a rise in the annealing temperature from 120 to 200 °C markedly increases from 26 ± 6 to 75 ± 8 nm. Changes in the size of particles formed inside grains are less pronounced, and their size increases from ≈4 to 11 nm. Following the data of recent works,[17,19] it can be assumed that the particles revealed in TEM images refer to the $MgZn_2$ phase.

It is important to note that such arrangement of secondary phase particles and differences in their sizes after annealing or artificial aging are also characteristic of other UFG aluminum-based alloys processed by SPD.[20,21] It is assumed that the segregations and clusters formed by dissolved atoms at grain boundaries and within ultrafine grain interior during HPT at RT may grow during annealing and transform into the $MgZn_2$ phase of stable modifications instead of the usual Guinier–Preston zone because of the accelerated grain-boundary diffusion and increased concentration of vacancies.

The observed evolution of the UFG structure after annealing correlates well with the nature of the change in alloy hardness (Figure 2). Therefore, annealing to a temperature of 120 °C, when the microstructural changes are minimal, the microhardness, HV, decreased slightly from 186 ± 7 to 170 ± 7. Further increase in the annealing temperature leading to coarsening of the UFG structure causes a monotonic decrease in the hardness. After annealing at 200 °C, the hardness of the UFG alloy reaches the value of 115 ± 6, closing to the hardness of the coarse-grained alloy hardened by conventional heat treatment T6. Summing up the obtained data on the evolution of the microstructure and hardness of the UFG alloy processed by HPT at RT, it can be assumed that the alloy may retain the high strength in the temperature range up to 170 °C.

3.2. Mechanical Properties at Room and Elevated Temperatures

The engineering stress–strain curves obtained at RT on the HPT-processed and conventionally T6-treated samples are shown in **Figure 3**a. Experimental results show that the strength characteristics ($\sigma_{YS} = 631 \pm 10$ MPa and $\sigma_{UTS} = 678 \pm 5$ MPa) of the HPT-processed samples are significantly higher than that after conventional heat treatment T6 ($\sigma_{YS} = 397 \pm 9$ MPa and $\sigma_{UTS} = 418 \pm 6$ MPa) or that after processing by equal channel angular pressing (ECAP) ($\sigma_{UTS} \approx 470$ MPa)[13] performed at RT on the same alloy. Considerable strength of the HPT-processed sample, which is comparable to the high strength of commercial alloy 7075 processed by high-pressure sliding (HPS),[22] is clearly related not only to the formation of a homogeneous UFG structure but also possible because of the formation of nanoclusters and atom segregations of the main alloying elements in the aluminum matrix.[12,18] According to the data in the studies given by Valiev et al. and Zhang et al.[14,18] the contribution of these nanosized elements may reach more than 15% of the total hardening.

At the same time, the increase in the strength of the material after HPT is accompanied by a noticeable decrease in ductility, especially in uniform elongation (from 10% to only 1.5%) as compared with the coarse-grained alloy after conventional heat treatment T6 (Figure 3a). Such change in ductility of the UFG materials under tension at RT is typical for many aluminum alloys subjected to SPD.[23–26] However, it should be noted that total elongation to failure ($\delta = 7.8\% \pm 0.4\%$) demonstrated by the UFG alloy in a high-strength state is acceptable for its practical application.

To study the superplastic behavior of the UFG alloy, static tensile tests were performed in the range of strain rates from 10^{-2} to $10^{-4}\,\mathrm{s}^{-1}$ and temperatures from 120 to 170 °C (0.43–0.48 T_{melt}). The choice for such temperature range was inspired by the analysis of the results on thermal stability studies of the UFG samples presented in the previous section.

Figure 3b shows typical stress–strain curves resulting from mechanical tests at 120 °C on the HPT-processed samples. It
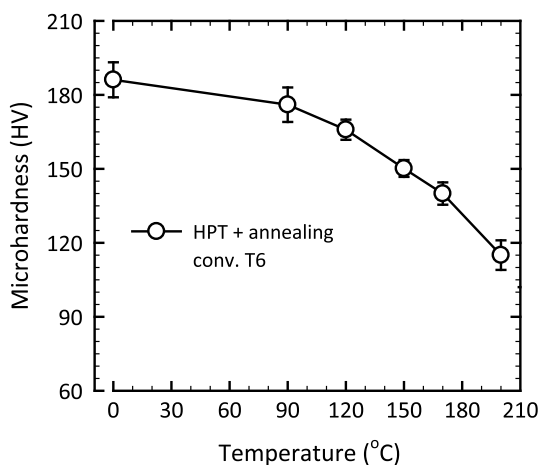
Figure 2. Dependence of microhardness in the UFG Al alloy after HPT at RT on temperature of annealing for 1 h.

**ADVANCED
SCIENCE NEWS**
www.advancedsciencenews.com

**ADVANCED
ENGINEERING
MATERIALS**
www.aem-journal.com
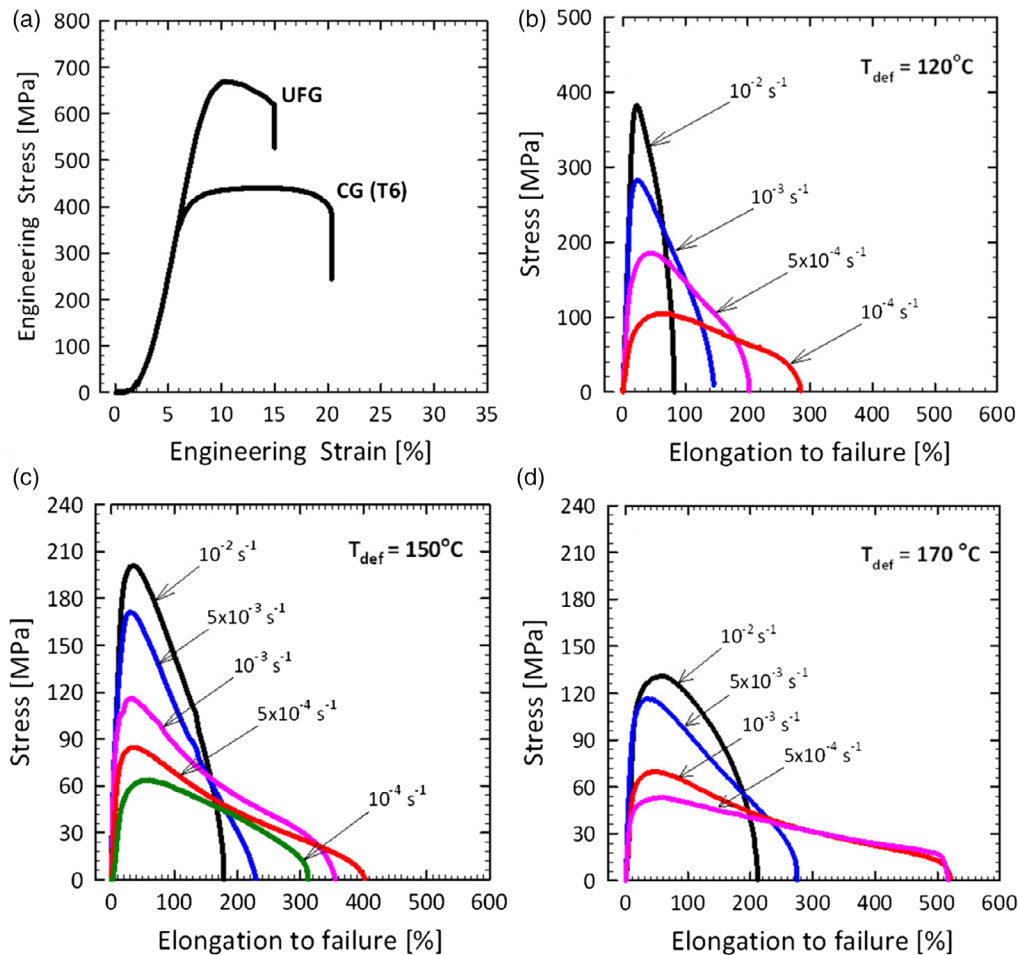
Figure 3. Engineering stress–strain curves for the UFG Al alloy. Tensile testing at a) RT, b) 120 °C, c) 150 °C, and d) 170 °C.

can be seen that the decrease in the strain rate is accompanied by a noticeable decrease in the flow stress and an increase in the ductility of the investigated material. The highest total elongation to failure (278%) and lowest maximum flow stress ($\sigma_{max} = 104$ MPa) were obtained at the initial strain rate of $10^{-4}\,s^{-1}$. The highest total elongations (400% and 490%) were observed at a test temperature of 150 °C and a strain rate of $5 \times 10^{-4}\,s^{-1}$ and at 170 °C and $10^{-3}\,s^{-1}$, respectively (Figure 3c,d).

According to the obtained experimental values, the dependences of total elongation and the maximum flow stress on the initial strain rate are plotted in **Figure 4**a. In addition, Figure 4b shows the values of strain rate sensitivity, m, obtained in different conditions. It can be seen that an increase in the test temperature leads to a decrease in the flow stress and to a shift of the maximum ductility to a range of higher strain rates. A decrease in the strain rate at temperatures of 150 and 170 °C from 5×10^{-4} to $10^{-4}\,s^{-1}$ leads to a decrease in both the flow stress and ductility. Such features of mechanical behavior were also observed on other superplastic materials with UFG structure.[27–31] In addition, for superplastic behavior of the UFG alloy, it is established that the maximum values of the strain

rate sensitivity, m, coincide with the temperature-rate test conditions under which the samples demonstrate the highest total elongations (Figure 4b).

It is important to note that such typical signs of SP as high values of parameter m ($\approx$0.45) and elongation to failure (278% and 400%) were recorded, for the first time, in high-strength UFG Al alloy at such low temperatures of 120 and 150 °C, where only slight softening of the HPT material after annealing was observed (Figure 2).

3.3. The Microstructure Evolution and Strength of the UFG Alloy after Superplastic Deformation

The consequences of tensile tests at 120 °C and an initial strain rate of $10^{-4}\,s^{-1}$, and at temperatures of 150 and 170 °C and a strain rate of $10^{-3}\,s^{-1}$ in the form of microhardness graphs are shown in **Figure 5**, representing the microhardness values at RT on the gauge length of the samples (close to fracture area). Under these temperature and rate conditions, the UFG alloy demonstrates superplastic behavior with high values of total elongation up to about 500% and high values of strain rate sensitivity ($m>0.4$). For comparison, Figure 5 also includes a
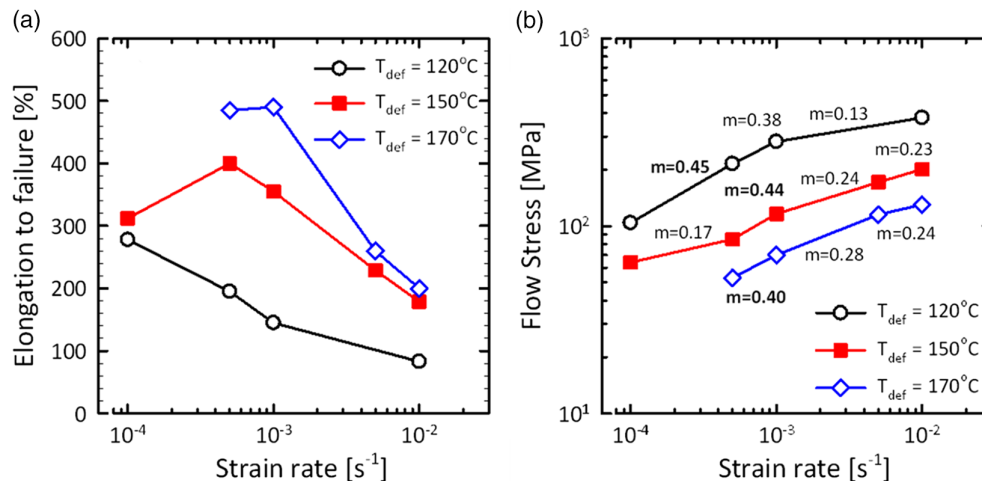
Figure 4. Dependence of a) total elongation and b) stress on strain rate following the results of tensile tests at 120, 150, and 170 °C of UFG Al alloy.
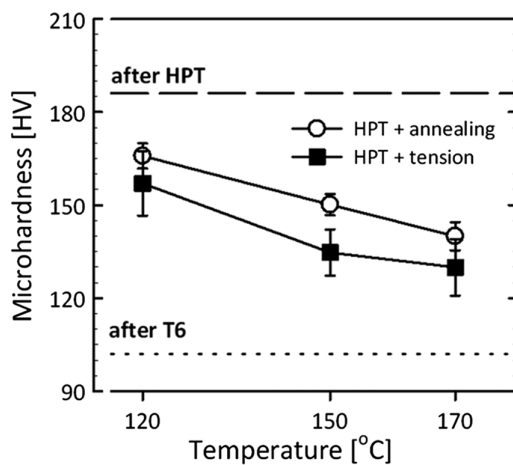
Figure 5. Dependence of microhardness in the UFG Al alloy on different temperatures of superplastic deformation (measured on the gauge length of the sample at a distance of 0.20 mm from the fracture area) and annealing for 1 h.

graph of microhardness change for the UFG alloy sample after annealing for 1 h at similar temperatures.

It is clear that when increasing the temperature of superplastic deformation, the change in the UFG alloy microhardness is of similar character as in the case of annealing for 1 h (Figure 5). Minimum softening can be observed. TEM studies of the UFG alloy structure (**Figure 6**) after superplastic deformation at a temperature of 170 °C and a strain rate of 10^{-3} s^{-1} showed a certain increase in the mean grain size to 338 ± 20 nm, but the grain shape remains equiaxial. Images of dispersed particles of the MgZn$_2$ phase resulting from deformation are shown in Figure 6b. Their morphology and distribution in the UFG alloy structure are qualitatively similar to the material after annealing (Figure 1d). Superplastic deformation includes elongation of samples by 100%, but the formation of high dislocation density within grain interior is not observed (Figure 6c,d). The absence of noticeable changes in the grain shape and the developed intragranular dislocation structure directly indicates that superplastic deformation of the UFG alloy Al–4.8Zn–1.2Mg–0.14Zr is caused by the mechanism of GBS.

It is important to note that despite certain softening after superplastic deformation of the UFG alloy with a tension of more than 300%, the material at RT retains a level of strength up to 50% higher than that after conventional heat treatment T6, when the effect of dispersion hardening is realized to the maximum extent.[16]

4. Discussion

The investigations conducted in this work made it possible to achieve new and exciting results concerning the SP in UFG materials.

First, it was established that the superplastic behavior in the UFG Al alloy of 7xxx series may be realized at quite low temperatures of 120–170 °C. At a temperature of 120 °C and a strain rate of 10^{-4} s^{-1}, the total elongation exceeds 250%, and at a temperature of 170 °C and a strain rate of 10^{-3} s^{-1}, it was about 500%. At the same time, a high strain rate sensitivity up to 0.45 was observed, which is typical for superplastic deformation. Conventionally, the 7xxx series alloys with a grain size in the micrometer range exhibited superplastic behavior at temperatures of 450–500 °C.[32,33] However, in earlier works,[8,9,34] superplastic behavior at lower temperatures of ≈250–300 °C revealed in several Al alloys was explained by the formation of the UFG structure with a grain size in the submicron range, in consequence of which the contribution of GBS increases significantly, which is, in turn, the main mechanism responsible for superplastic deformation.

Recent findings of SP phenomenon in ultrafine Al–Zn and Mg alloys at RT[11,35,36] showed the significance of another parameter, i.e., the grain boundary structure, toward the effect. Precise analysis with the use of TEM/HREM and 3D APT revealed the formation of segregations at grain boundaries in these alloys after SPD processing that accelerate the grain boundary diffusion and activate GBS. This mechanism is well confirmed experimentally.[11,37–40] There are high chances that

**ADVANCED
SCIENCE NEWS**
www.advancedsciencenews.com

**ADVANCED
ENGINEERING
MATERIALS**
www.aem-journal.com
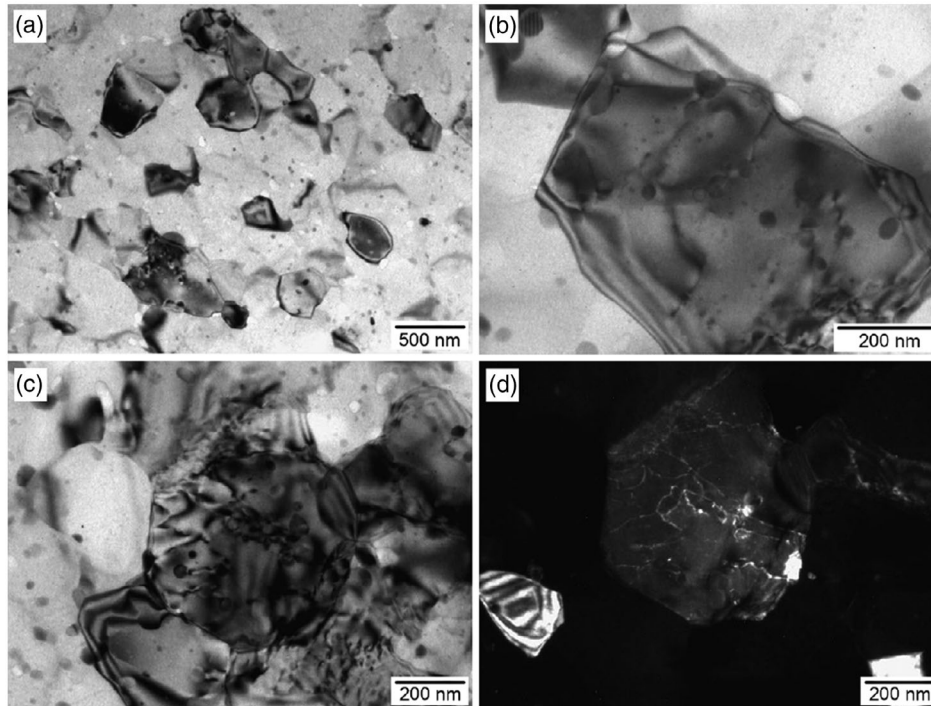
Figure 6. TEM images of microstructure in the gauge length of the UFG Al alloy sample after superplastic deformation at 170 °C, 10^{-3} s^{-1}: a–c) bright field and d) dark field.

HPT similarly causes the formation of Zn segregations at grain boundaries in the UFG alloy Al–Zn–Mg studied in this work; such segregations activating GBS lead to a decrease in the temperature of SP effect. However, this assumption calls for additional experimental studies that the authors plan to perform in near future.

Another new important result revealed in this work is the observation of very high strength in the UFG alloy at RT, and the strength value remains high even after superplastic deformation. This fact is unusual because, typically, the material after superplastic deformation exhibits lower strength and requires additional thermomechanical treatment for its increase.[32,33] In this case, the strength of the UFG alloy after superplastic deformation is still considerably higher than that after conventional heat treatment T6 (Figure 5). As it is noted in Section 3.3, there are several reasons for this phenomenon. First, after superplastic deformation at lower temperature, the shape and size of grains do not noticeably change, and the contribution of the ultrafine grain size to the alloy hardening is significant. Besides, additional hardening is caused by nanosized particles of the secondary phase that are present in the structure of the UFG alloy (Figure 6b). Furthermore, recent experiments prove that segregations activating GBS also may lead to strengthening at lower straining temperatures or providing the presence of various types of atoms to form segregations.[14,38] In general, maintaining the high-strength state of the alloy after superplastic deformation at low temperatures is of practical importance, as it is of direct interest for the development of new technological processes of superplastic forming of complex-shaped products with high-strength and service properties.[41]

5. Conclusion

The obtained results for this work can be summarized as follows: 1) The application of HPT processing contributes to the formation of homogeneous UFG structure in the alloy Al–Zn–Mg–Zr under study with a mean grain size of ≈170 nm that remains sufficiently stable up to the temperatures of 120–150 °C. After annealing at higher temperatures, a slight grain growth occurs and the appearance of nanosized precipitates of the second phase 15–30 nm in size is observed in the structure. 2) The investigated UFG alloy demonstrates a very high strength at RT (σ_{UTS} higher than 670 MPa), and, at a temperature of 120–150 °C, it exhibits a typical superplastic behavior but maintains a high-strength state under normal conditions after superplastic deformation. 3) The superplastic behavior of the UFG alloy at such low temperatures may be caused by the presence of grain-boundary zinc segregations that activate the development of GBS and contribute to the exhibition of the SP effect. 4) The combination of RT SP in the alloy while maintaining its high-strength state may become an object of close attention for the industry as this phenomenon offers new perspectives for the development of new technological processes of superplastic forming of complex-shaped items with high service properties.

In general, the results of this work demonstrate that the interest in SP of the UFG materials—the subject area where Langdon is the world-famous expert and author of many pioneering results—remains extremely high, and superplastic materials are further developed to identify opportunities and need for future fundamental research as well as to identify the potential for commercial application and ways of cheaper manufacturing of such materials.

[1] H. Ishikawa, D. G. Bhat, F. A. Mohamed, T. G. Langdon, *Metall. Trans.* **1977**, *8A*, 523.

[2] M. M. I. Ahmed, T. G. Langdon, *Metall. Trans.* **1977**, *8A*, 1832.

[3] T. G. Langdon, *Metall. Mater. Trans. A* **1982**, *13A*, 689.

[4] A. H. Chokshi, A. K. Mukherjee, T. G. Langdon, *Mater. Sci. Eng. R* **1993**, *10*, 237.

[5] T. G. Langdon, *J. Mater. Sci.* **2009**, *44*, 5998.

[6] R. B. Vastava, T. G. Langdon, *Acta Metall* **1979**, *27*, 251.

[7] T. G. Langdon, *Acta Metall. Mater.* **1994**, *42*, 2437.

[8] R. Z. Valiev, O. A. Kaibyshev, R. I. Kuznetsov, R. Sh. Musalimov, N. K. Tsenev, *Dokl. Akad. Nauk. SSSR* **1988**, *301*, 864.

[9] R. Z. Valiev, A. V. Korznikov, R. R. Mulyukov, *Mater. Sci. Eng. A* **1993**, *A168*, 141.

[10] R. Z. Valiev, D. A. Salimonenko, N. K. Tsenev, P. Berbon, T. Langdon, *Scripta Mater.* **1997**, *37*, 1945.

[11] R. Z. Valiev, M. Yu. Murashkin, A. Kilmametov, B. Straumal, N. Q. Chinh, T. G. Langdon, *J. Mater. Sci.* **2010**, *45*, 4718.

[12] J. Gubicza, I. Schiller, N. Q. Chinh, J. Illy, Z. Horita, T. G. Langdon, *Mater. Sci. Eng. A* **2007**, *460-461*, 77.

[13] Z. C. Duan, N. Q. Chinh, C. Xu, T. G. Langdon, *Metall. Mater. Trans. A* **2010**, *41A*, 802.

[14] R. Z. Valiev, N. A. Enikeev, M. Yu. Murashkin, V. U. Kazykhanov, X. Sauvage, *Scripta Mater* **2010**, *63*, 949.

[15] E. V. Bobruk, M. Y. Murashkin, V. U. Kazykhanov, R. Z. Valiev, *Adv. Eng. Mater.* **2019**, *21*, 1800094.

[16] A. Azarniya, A. K. Taheri, K. K. Taheri, *J. Alloys Compd.* **2019**, *781*, 945.

[17] Y. Zhang, S. Jin, P. W. Trimby, X. Liao, M. Y. Murashkin, R. Z. Valiev, J. Liu, J. M. Cairney, S. P. Ringer, G. Sha, *Acta Mater.* **2019**, *162*, 19.

[18] Y. Zhang, S. Jina, P. Trimby, X. Liao, M. Y. Murashkin, R. Z. Valiev, G. Sha, *Mater. Sci. Eng. A* **2019**, *752*, 223.

[19] M. V. Markushev, E. V. Avtokratova, S. V. Krymskiy, O. Sh Sitdikov, *J. Alloys Compd.* **2018**, *743*, 773.

[20] M. Murashkin, I. Sabirov, V. Kazykhanov, E. Bobruk, A. Dubravina, R. Z. Valiev, *J. Mater. Sci.* **2013**, *48*, 13.

[21] X. Sauvage, E. V. Bobruk, M. Yu. Murashkin, Y. Nasedkina, N. A. Enikeev, R. Z. Valiev, *Acta Mater.* **2015**, *98*, 355.

[22] S. Lee, K. Tazoe, I. F. Mohamed, Z. Horita, *Mater. Sci. Eng. A* **2015**, *628*, 56.

[23] I. Sabirov, M. Yu. Murashkin, R. Z. Valiev, *Mater. Sci. Eng. A* **2013**, *560*, 1.

[24] E. C. Moreno-Valle, I. Sabirov, M. T. Perez-Prado, M. Yu. Murashkin, E. V. Bobruk, R. Z. Valiev, *Mater. Lett.* **2011**, *65*, 2917.

[25] G. Sha, K. Tugcu, X. Z. Liao, P. W. Trimby, M. Y. Murashkin, R. Z. Valiev, S. P. Ringer, *Acta Mater.* **2014**, *63*, 169.

[26] Y. Liu, M. Liu, X. Chen, Y. Cao, H. J. Roven, M. Murashkin, R. Z. Valiev, H. Zhou, *Scripta Mater.* **2019**, *159*, 137.

[27] R. Z. Valiev, R. K. Islamgaliev, I. P. Semenova, *Mater. Sci. Eng. A* **2007**, *463*, 2.

[28] S. V. Dobatkin, E. N. Bastarache, G. Sakai, T. Fujita, Z. Horita, T. G. Langdon, *Mater. Sci. Eng. A* **2005**, *408*, 141.

[29] G. Sakai, Z. Horita, T. G. Langdon, *Mater. Sci. Eng. A* **2005**, *393*, 344.

[30] M. Kawasaki, T. G. Langdon, *J. Mater. Sci.* **2016**, *51*, 19.

[31] M. Kawasaki, T. G. Langdon, *Rev. Adv. Mater. Sci.* **2018**, *54*, 46.

[32] O. A. Kaibyshev, *Superplasticity of Alloys Intermetallides and Ceramics*, Springer-Verlag, Berlin **1992**.

[33] T. G. Nieh, J. Wadsworth, O. D. Sherby, *Superplasticity in Metals and Ceramics,*, Cambridge University Press, Cambridge, UK **1997**.

[34] S. X. McFadden, R. S. Mishra, R. Z. Valiev, A. P. Zhilyaev, A. K. Mukherjee, *Nature* **1999**, *398*, 684.

[35] K. Edalati, Z. Horita, R. Z. Valiev, *Sci. Rep.* **2018**, *8*, 6740.

[36] K. Edalati, T. Masuda, M. Arita, M. Furui, X. Sauvage, Z. Horita, R. Z. Valiev, *Sci. Rep.7* **2017**, *2662*, 1.

[37] N. Q. Chinh, T. Csanádi, T. Győri, R. Z. Valiev, B. B. Straumal, M. Kawasaki, T. G. Langdon, *Mater. Sci. Eng. A* **2012**, *543*, 117.

[38] X. Sauvage, G. Wilde, S. V. Divinski, Z. Horita, R. Z. Valiev, *Mater. Sci. Eng. A* **2012**, *540*, 1.

[39] N. Q. Chinh, R. Z. Valiev, X. Sauvage, G. Varga, K. Havancsák, M. Kawasaki, B. B. Straumal, T. G. Langdon, *Adv. Eng. Mater.* **2014**, *16*, 1000.

[40] N. Q. Chinh, P. Jenei, J. Gubicza, E.V. Bobruk, R.Z. Valiev, *Mater. Lett.* **2017**, *186*, 334.

[41] A.J. Barnes, *Mater. Sci. Forum* **2001**, *357—359*, 3.